ARTICLES

Two-Body Dissociative Charge Exchange Dynamics of *sym*-Triazine

John D. Savee, Jennifer E. Mann, and Robert E. Continetti*

Department of Chemistry and Biochemistry, University of California at San Diego, 9500 Gilman Drive, La Jolla, California 92093-0340

Received: February 17, 2009; Revised Manuscript Received: May 19, 2009

Translational spectroscopy coupled with coincidence detection techniques has been used to investigate the two-body dissociation of *sym*-triazine to HCN + $(HCN)_2$ upon electronic excitation from charge exchange between the *sym*-triazine cation and cesium. This dissociation mechanism was determined to occur after excitation of *sym*-triazine into the 3s Rydberg electronic manifold, and the observed dynamics suggest that the mechanism competes with a stepwise three-body dissociation mechanism to three HCN products that occurs from this same electronic excitation. On the basis of reported stabilization energies of several isomers of the HCN dimer, possible structures of the metastable $(HCN)_2$ species are discussed in light of the current measurements.

1. Introduction

Owing to its stability, the hydrogen cyanide (HCN) molecule is ubiquitous in nature—HCN and its oligomers are believed to play a role in a variety of environments ranging from synthesis of organic species in prebiotic atmospheres to the chemistry of dark interstellar clouds.[1,2] In particular, dimerization of HCN has been the focus of a considerable amount of previous work. Production of $(HCN)_2$ using a variety of methods (e.g., matrix isolation,[3−5] molecular beams,[6,7] and in helium droplets[8]) have yielded weakly bound hydrogen-bonded structures which have been confirmed by accompanying ab initio investigations.[9,10] Although never experimentally detected, a cyclic diazete form of the HCN dimer (1,3-diazete) has been the focus of several ab initio studies, largely due to it being an aza-substituted derivative of cyclobutadiene.[11−16] Experimental studies by Evans et al.[17] and Jobst et al.[18] identified several covalent isomers of the HCN dimer (denoted as $C_2N_2H_2$) as stable in the gas-phase, and used ab initio techniques to determine their relative stabilities. The experimentally identified $C_2N_2H_2$ species *C*-cyanomethanimine (both Z and E conformers), *N*-cyanomethanimine, aminocyanocarbene, and ethenediimine, along with 1,3-diazete are shown in Figure 1 with their calculated stabilization energies relative to 2HCN (E_{rel}) as reported in refs 15, 17, and 18. As shown by the stabilization energies, some of these isomers are nearly isoenergetic with 2HCN while others represent local minima on the $C_2N_2H_2$ reaction coordinate at higher energies.

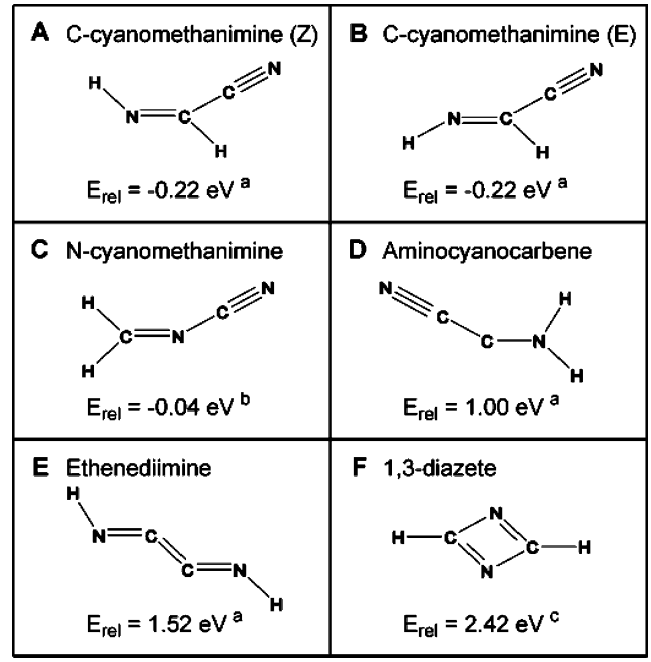

Figure 1. Various isomers of $C_2N_2H_2$ that have been identified in the gas phase, along with 1,3-diazete which has been considered as a potential intermediate in the dissociation of Tz. Their energies relative to 2HCN (E_{rel}) were calculated using various ab initio methods as reported in refs 15(c),17(b), and 18(a).

In several recent investigations the chemistry of electronically excited *sym*-triazine (Tz), a heterocyclic trimer of HCN, has been probed by observation of dissociation products using translational spectroscopy coupled with coincidence detection techniques.[19−21] These previous works focus on the three-body decomposition of Tz (→3HCN) upon electronic excitation via charge exchange (CE) of the *sym*-triazine cation (Tz^+) with a cesium electron donor. Using this method, it was observed that excitation into different electronic manifolds results in unique dissociation mechanisms; excitation of Tz into the $\pi^* \leftarrow n$ manifold of states results in a concerted three-body mechanism, while excitation into the 3s Rydberg manifold of states ($R_s \leftarrow n$) yields a stepwise mechanism implying a short-lived $(HCN)_2$ intermediate. Interestingly, excitation of Tz using CE also yielded a two-body HCN + $(HCN)_2$ product channel that was observable in the time scale of the experiment implying an

* To whom correspondence should be addressed. E-mail: rcontinetti@ucsd.edu.

10.1021/jp901462d CCC: $40.75
Published on Web 07/10/2009

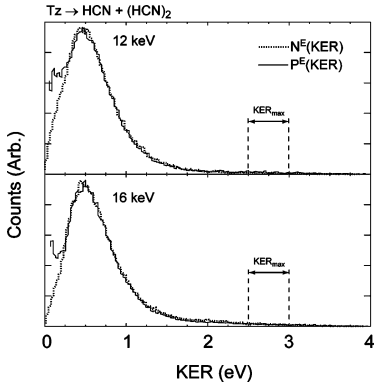

Figure 2. Measured N^E(KER) and calculated P^E(KER) distributions (in eV) for the HCN $+(HCN)_2$ two-body dissociation of 12 and 16 keV Tz^+ beams upon CE with Cs. The maximum observed KER for this product channel occurs between 2.5 and 3.0 eV, as indicated by the region labeled KER_{max}.

$(HCN)_2$ lifetime of >6.5 μs. Previous translational spectroscopy experiments invoking $\pi^* \leftarrow n$ and $\pi^* \leftarrow \pi$ transitions via photolysis of neutral Tz did not observe this product channel, implying that this mechanism did not occur from those locales on the Tz potential energy surface (PES), the lifetime of the $(HCN)_2$ intermediate was short on the time scale of their experiments (hundreds of microseconds), or $(HCN)_2$ did not survive the reionization process required for their TOF measurements of the reaction products.[22,23] This two-body channel is the primary focus of this manuscript, and will be discussed in light of previous insight into the stability of $C_2N_2H_2$ along with past conclusions regarding the resulting dynamics from excitation of Tz via the CE process.

2. Experimental Section

Essential aspects of the coincidence experiment involving CE of fast 12 and 16 keV beams of Tz^+ with Cs have been presented elsewhere.[19−21] Two-body coincidence data for dissociation of Tz to masses 54 and 27 au were collected concurrently with data for the three-body product channel (Tz → 3HCN), allowing the determination of a branching ratio between the two- and three-body channels. Empirical product kinetic energy release (KER) distributions, N^E(KER), were constructed using the raw time and position data collected at each beam energy. On account of the finite size of the neutral particle detector, a correction employing Monte Carlo (MC) simulations of the detector's geometric collection efficiency[24] was applied to empirical N^E(KER) distributions to obtain P^E(KER) probability distributions.

3. Results

The measured N^E(KER) (dotted trace) and resulting P^E(KER) (solid trace) distributions obtained for dissociation of Tz to HCN $+ (HCN)_2$ upon CE of 12 and 16 keV beams of Tz^+ with Cs are shown in Figure 2. At both beam energies the P^E(KER) spectrum is characterized by a broad distribution peaked near 0.50 eV with a tail extending toward the high-energy side of the spectrum. Because nonresonant excitation of Tz is possible via the CE mechanism, the available energy (E_{avl}) must be determined in an ad hoc manner based on experimental observations.[19,20,25] Assuming that some products are produced with no internal excitation, the available energy above the HCN $+ (HCN)_2$ dissociation limit can be estimated from the maximum observed KER (KER_{max}) in the P^E(KER) spectrum. Due to the gradual diminishment of the tail in the HCN $+ (HCN)_2$ P^E(KER) spectra, KER_{max} is estimated to lie between 2.5 and 3 eV. The value of <KER> for the 16 keV P^E(KER) distribution was calculated to be 0.56 eV, and occurs near the 0.50 eV peak in the spectrum. Under the aforementioned assumption regarding the relationship between KER_{max} and E_{avl}, the average internal energy imparted to the fragments (<E_{int}>) is estimated to be between 1.94 and 2.44 eV, or, ∼80% of E_{avl}. The transition probability for nonresonant excitation into vibronic states of neutral molecules via CE is well-known to vary nonlinearly with the relative velocity between the cation and electron donor (e.g., with beam energy).[19,20,25,26] The invariance of the P^E(KER) spectrum with the beam energy implies that a single electronic excitation of Tz gives rise to dissociation to HCN + $(HCN)_2$; a thorough discussion of the origin of this mechanism on the Tz PES will be provided in Section 4.

Branching fractions (χ_j) were also obtained for the competing two- and three-body product channels observed in the present experiment using eq 1:

$$\chi_j = \frac{Z^{-n_j} \cdot \int P_j^E(\mathrm{KER}) \cdot \mathrm{dKER}}{\sum_j Z^{-n_j} \cdot \int P_j^E(\mathrm{KER}) \cdot \mathrm{dKER}} \quad (1)$$

Here, the index j denotes a given product channel and $\int P_j^E(\mathrm{KER}) \cdot \mathrm{dKER}$ is the number of counts in the associated probability distribution for that channel. The term Z^{-n_j} in eq 1 accounts for the detection efficiency for a single particle by the MCP detector. Here Z, the absolute detection efficiency of the incident MCP on the neutral particle detector, is estimated as $Z = 0.5$ and n_j is equal to the number of fragments produced in product channel j.[27] In the present experiment, the two-body channel was found to occur with branching fractions of 0.28 ± 0.03 and 0.26 ± 0.03 at 12 and 16 keV beam energies, respectively. This branching fraction does not vary significantly in regard to the center-of-mass flight time to the neutral particle detector after neutralization at the different beam velocities (6.5 and 5.6 μs for 12 and 16 keV cation beams, respectively), and implies a lifetime of at least 6.5 μs for the observed $(HCN)_2$ species.

4. Discussion

Assignment of the initial Tz state leading to HCN + $(HCN)_2$ production is straightforward in light of previous investigations into the dissociation dynamics of Tz induced by CE of Tz^+ with Cs. In these previous investigations, the generalized Mulliken−Hush (GMH) approach[28] was used to calculate the coupling of initial and final states in the CE of Tz^+ with Cs (i.e., $[Tz^+ \cdots Cs]$ with $[Tz^* \cdots Cs^+]$ where Tz* represents various electronically excited states of Tz).[19,20] Using the GMH method and the two-state Demkov model for nonadiabatic transitions,[26] it was concluded that the CE process had a propensity for populating Tz in vibronic states within the $\pi^* \leftarrow n$ and $R_s \leftarrow n$ (3s Rydberg) electronic manifolds. The energies of these vibronic states as determined by KER_{max} values in the three-body product channel (4 and 5 eV above the 3HCN dissociation limit for the $\pi^* \leftarrow n$ and $R_s \leftarrow n$ excitations, respectively) are indicated in Figure 3. The GMH coupling for capture of an electron into the $R_s \leftarrow n$ manifold was found to be significantly greater than that for capture into the $\pi^* \leftarrow n$ manifold. This, coupled with the considerable branching fraction associated with the two-body product channel (>0.25), leaves little doubt that

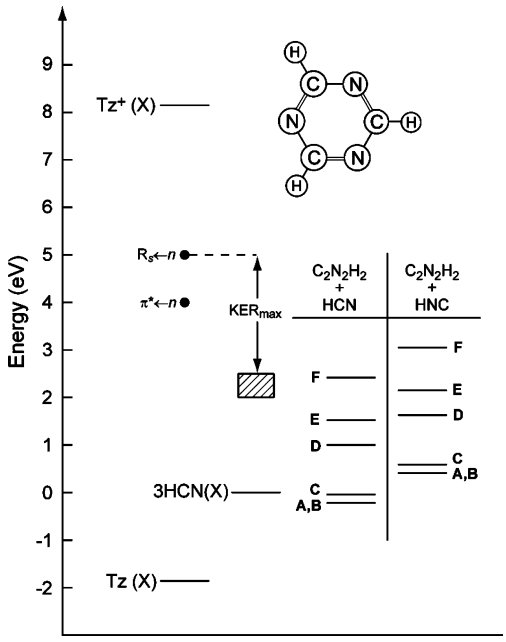

Figure 3. Schematic energy level diagram for the two-body dissociation of Tz to HCN + $(HCN)_2$. The black dots labeled $R_s \leftarrow n$ and $\pi^* \leftarrow n$ are the excitation energies for these electronic manifolds of Tz upon CE of Tz^+ with Cs as determined from analysis of the three-body dissociation dynamics of Tz in refs 19−21 (at 5 and 4 eV relative to 3HCN, respectively). The dissociation limits for production of HCN or HNC and various $C_2N_2H_2$ isomers shown on the right side of the diagram correspond to the structures and values of E_{rel} provided in Figure 1.

the HCN + $(HCN)_2$ product channel is the result of an initial $R_s \leftarrow n$ excitation of Tz.

The doubly degenerate $R_s \leftarrow n$ electronic manifold (E') has been found to undergo Jahn−Teller distortion (E⊗e) resulting in a "Mexican hat"-type potential surface with minima at C_{2v} symmetry and a conical intersection at D_{3h} symmetry. Previous investigations into the three-body dissociation dynamics of Tz upon CE of Tz^+ with Cs have suggested that a vibronic state populated in a lower energy region of this manifold of states gives rise to a stepwise dissociation mechanism (eq 2).

$$Tz^* \rightarrow HCN + (HCN)_2 \rightarrow 3HCN \qquad (2)$$

If different vibronic states within this electronic manifold were responsible for the two- and three-body mechanisms, then it would be reasonable to expect different couplings for the CE process, and thus a changing two- to three-body branching fraction as the cation beam velocity is varied. Because the branching fraction between the two- and three-body channels does not appear to vary significantly with beam energy, we operate under the assumption that the two-body mechanism competes with the stepwise three-body mechanism upon excitation into a single $R_s \leftarrow n$ state of Tz.

On the basis of these conclusions, there are two simple reaction paths that can be used to represent competing 3HCN and HCN + $(HCN)_2$ mechanisms from a common origin on the Tz PES. In the first case, the two-body mechanism proceeds through a completely separate reaction coordinate than the stepwise three-body mechanism upon excitation of Tz. In the second case, a common reaction coordinate is initially shared through ejection of a single HCN fragment, but subsequently diverges resulting in either metastable $(HCN)_2$ or 2HCN. In a previous investigation into the dynamics of the stepwise dissociation mechanism accessed in this experiment, ad hoc MC simulations employing a simple two-step model of stepwise dissociation were able to reasonably reproduce the experimentally observed dynamics.[21] The "best fit" of this model to experimental data occurred when the total KER (KER_{tot}) was partitioned such that 25% of KER_{tot} was associated with dissociation of Tz to HCN + $(HCN)_2$. In the three-body P^E(KER) spectrum, $\langle KER_{tot} \rangle$ for the stepwise mechanism was determined to be ∼2.6 eV. If this value is the result of a two-step process that behaves according to the MC model predictions, then using $\langle KER_{tot} \rangle$ for KER_{tot} yields the prediction of a 0.65 eV KER (25% of KER_{tot}) in the first step of the stepwise mechanism. This value is reasonable agreement with the <KER> measured for the two-body channel (0.56 eV), and suggests a common reaction coordinate for the stepwise three-body mechanism and the two-body channel through the ejection of the first HCN fragment (thus favoring the second proposed reaction path).

A major point of interest raised by this experiment regards the nature of the detected $(HCN)_2$ species from the observed energetics and dynamics accompanying dissociation of Tz after excitation in the $R_s \leftarrow n$ manifold. The observed range of $\langle E_{int} \rangle$ = 1.94−2.44 eV includes the total internal energy for all dissociation products, and thus marks an upper bound for the average internal energy carried away by $(HCN)_2$. Goates et al. measured infrared emission from the ν_2 (bend) and ν_3 (C−H stretch) modes of HCN produced by 193 nm photolysis of Tz (most likely originating from a $\pi^* \leftarrow \pi$ transition) and found that the number of quanta deposited in bend excitation exceeded that for C−H stretch excitation by a factor of 70.[29] Although dissociation from an $R_s \leftarrow n$ vibronic state proceeds along a different reaction coordinate, we qualitatively assume that HCN produced from any excitation of Tz will carry away a significant degree of bend excitation due to its highly strained orientation in the Tz ring structure. While the HCN fragment quite possibly receives a large portion of the total internal energy measured in this experiment, we cannot exclude the possibility that $(HCN)_2$ is formed with enough internal energy to overcome barriers to isomerization.

In past CE experiments, we have used the measured KER_{max} from P^E(KER) distributions to identify the energetic location of the unknown initial excited state on the neutral PES relative to a known dissociation limit. In the case of dissociation of Tz to HCN + $(HCN)_2$, the exact opposite is known and unknown−dissociation is assumed to proceed from a known excited state leading to products with an unknown dissociation limit. In the three-body Tz experiment it was determined that the $R_s \leftarrow n$ state accessed lies ∼5 eV above the 3HCN dissociation limit (6.86 eV above the Tz ground state). Projecting downward energetically from this state by the KER_{max} range observed in the present experiment, we can estimate an energetic region where the HCN+$(HCN)_2$ dissociation limit is expected to lie in the absence of radiative decay. This energetic region, indicated by a hatched box in Figure 3, is 2.0−2.5 eV above the 3HCN dissociation limit.

Dyakov et al. have investigated three-body reaction mechanisms of Tz using ab initio and RRKM techniques.[30] These studies suggest that at higher excitation energies cleavage of a C−N bond in the Tz ring structure may occur, leaving an open-ring biradical intermediate. Further decomposition through cleavage of a second C−N bond will produce HCN and a metastable open-ring biradical $(HCN)_2$ species. Although a very small barrier to dissociation was predicted for this $(HCN)_2$

intermediate (0.1 kcal/mol), the study by Dyakov et al. focused on the three-body dynamics of Tz and did not investigate the possibility of further stabilization of this intermediate. Due to the large amount of product internal energy in the present experiment, isomerization of this $(HCN)_2$ intermediate should be entertained. On the basis of the previously reported stabilization energies, dissociation limits can be determined for HCN plus several of the experimentally identified covalent $C_2N_2H_2$ species from Figure 1 (including 1,3-diazete), and are included in Figure 3. Although Goates et al. did not detect conclusive evidence for hydrogen isocyanide (HNC) production upon 193 nm photolysis of Tz ($\pi^* \leftarrow n$ or $\pi^* \leftarrow \pi$), a similar measurement has not been obtained for the dissociation products resulting from the higher-lying $R_s \leftarrow n$ excitation so we must consider its possible role in the present experiment.[29] The singlet ground state of HNC is endoergic with respect to HCN by ~0.63 eV, and thus the set of dissociation limits leading to HNC + $C_2N_2H_2$ in Figure 3 are the same as those for HCN + $C_2N_2H_2$ but offset to higher energy by this amount.[31] Clearly only two dissociation limits lie within the region predicted by the present experiment—the limit corresponding to HCN accompanied by 1,3-diazete (structure F in Figure 1) and the limit for production of HNC and ethenediimine (structure E in Figure 1).

It is not immediately clear which of these two potential sets of dissociation products is more likely. The argument for production of HNC and ethenediimine benefits from experimental observation that both species can be produced in at least a metastable state. However, dissociation of Tz via this channel would require significant rearrangement of the $(HCN)_2$ biradical resulting from ring-opening of Tz. Ethenediimine is a dimer of HNC covalently bound through terminal carbon atoms and thus isomerization would not only require migration of the three H-atoms from carbon to the nitrogen atoms, but would also require significant rearrangement of the heavy carbon and nitrogen atoms from their C−N arrangement in the Tz structure. Ab initio calculations by Jobst et al. suggest a barrier of 20 kcal/mol (~0.87 eV) for dissociation of ethenediimine to 2HNC, making it feasible that this species is identified as at least a metastable species in the present experiment.[18]

Arguments for the production of 1,3-diazete and HCN have a mechanistic simplicity but suffer from both a lack of experimental evidence for the 1,3-diazete species along with any thorough theoretical investigation into its ground state PES and dissociation energy. In the simplest picture, 1,3-diazete can be formed by a ring-closing isomerization of the biradical $(HCN)_2$ connecting the N and C termini where the two unpaired electrons are initially localized. This picture also offers a connection to the observed branching fraction for the two- and three-body product channels. As mentioned previously, the observed two-body KER appears to have a correlation with the stepwise three-body mechanism which suggests that they proceed along a similar reaction path through the ejection of the first HCN fragment. If competition between these two channels occurs from the open-ring biradical $(HCN)_2$, then it is within reason to assume that closure of the ring to form 1,3-diazete would be more likely to proceed from a singlet biradical (terminal electrons with opposite spin) rather than a triplet biradical (terminal electrons with the same spin). The resistance of the triplet $(HCN)_2$ biradical to ring closure may make it a more reasonable candidate for further decomposition (e.g., ultimately proceeding through the three-body channel). The measured branching fraction indeed shows that the three-body channel (which has been qualitatively shown to be dominantly comprised of signal resulting from $R_s \leftarrow n$ excitation[19−21]) is preferred in a 3:1 ratio to the two-body channel, supporting this type of statistical interplay of singlet and triplet states. Of course, this raises several issues regarding spin allowed dissociation paths (HCN must be produced in its ground singlet state), but a process like this involves complex nonadiabatic dynamics (e.g., biradicals are expected to be formed in excited states that can undergo intersystem crossing, the couplings for which are unknown in the present case), and this provides merely one simple explanation for the branching fraction observed in this experiment.

5. Conclusions

In addition to a three-body dissociation channel, excitation of Tz via CE with Cs results in a two-body channel, producing fragments with masses of 27 and 54 au that are stable for at least 6.5 μs in the present translational spectroscopy and coincidence measurement experiment. In light of previous investigations into the excitation of Tz using CE, this two-body mechanism likely results from the same $R_s \leftarrow n$ excitation that gives rise to a stepwise three-body mechanism. Correlation between the observed P^E(KER) spectrum for the two-body channel and the dynamics of the stepwise three-body mechanism suggest that they proceed along a common reaction coordinate through ejection of a single HCN fragment. Possible structures of the observed $(HCN)_2$ product were investigated in light of previous studies of stable isomers of $C_2N_2H_2$, although the conclusion that the most likely product channels are HNC + ethenediimine or HCN + 1,3-diazete would benefit from further investigation into lifetimes of these $C_2N_2H_2$ species. The proposed mechanism involves only species that have been previously identified in the gas-phase or, in the case of 1,3-diazete, suggested as potential intermediates in Tz dissociation, and further studies of two-body dissociation pathways of Tz would be of great interest. A thorough theoretical investigation into the PES of 1,3-diazete would, in particular, be of considerable use to the present study, as the inherent difficulty in handling the multiconfigurational nature of its ground state has limited all previous studies available in the literature.

Acknowledgment. This work was supported by the U.S. Air Force Office of Scientific Research under Grant No. FA9550-04-1-0035. The authors would like to thank A. I. Krylov and V. A. Mozhayskiy for their collaboration on the present work, as well as M. A. Fineman for his many contributions to this research.

References and Notes

(1) Heinrich, M. N.; Khare, B. N.; McKay, C. P. *Icarus* **2007**, *191*, 765.
(2) Irvine, W. M.; Schloerb, F. P *Astrophys. J.* **1984**, *282*, 516.
(3) King, C. M.; Nixon, E. R. *J. Chem. Phys.* **1968**, *48*, 1685.
(4) Satoshi, K.; Takayanagi, M.; Nakata, M. *J. Mol. Struct.* **1997**, *413*, 365.
(5) Pacansky, J. *J. Phys. Chem.* **1977**, *81*, 2240.
(6) Jucks, K. W.; Miller, R. E. *J. Chem. Phys.* **1988**, *88*, 6059.
(7) Jucks, K. W.; Miller, R. E. *Chem. Phys. Lett.* **1988**, *147*, 137.
(8) Nauta, K.; Miller, R. E. *J. Chem. Phys.* **1999**, *111*, 3426.
(9) Kofranek, M.; Karpfen, A.; Lischka, H. *Chem. Phys.* **1987**, *113*, 53.
(10) Kofranek, M.; Lischka, H.; Karpfen, A. *Mol. Phys.* **1987**, *61*, 1519.
(11) Glukhovtsev, M. N.; Simkin, B. Y.; Minkin, V. I. *J. Struct. Chem.* **1987**, *28*, 483.
(12) Bonacickoutecky, V.; Schoffel, K.; Michl, J. *J. Am. Chem. Soc.* **1989**, *111*, 6140.
(13) Facelli, J. C. *Theochem-J. Mol. Struct.* **1991**, *82*, 119.
(14) Politzer, P.; Grice, M. E.; Murray, J. S.; Seminario, J. M. *Can. J. Chem.-Rev. Can. Chim.* **1993**, *71*, 1123.
(15) Pai, S. V.; Chabalowski, C. F.; Rice, B. M. *J. Phys. Chem.* **1996**, *100*, 5681.

(16) Baric, D.; Maksic, Z. B. *J. Phys. Org. Chem.* **2003**, *16*, 753.
(17) Evans, R. A.; Lorencak, P.; Ha, T. K.; Wentrup, C. *J. Am. Chem. Soc.* **1991**, *113*, 7261.
(18) Jobst, K. J.; Hanifa, M. R.; Terlouw, J. K. *Chem. Phys. Lett.* **2008**, *462*, 152.
(19) Savee, J. D.; Mozhayskiy, V. A.; Mann, J. E.; Krylov, A. I.; Continetti, R. E. *Science* **2008**, *321*, 826.
(20) Mozhayskiy, V. A.; Savee, J. D.; Mann, J. E.; Continetti, R. E.; Krylov, A. I. *J. Phys. Chem. A* **2008**, *112*, 12345.
(21) Savee, J. D.; Mann, J. E.; Continetti, R. E. *J. Phys. Chem. A* **2009**, *113*, 3988.
(22) Ondrey, G. S.; Bersohn, R. *J. Chem. Phys.* **1984**, *81*, 4517.
(23) Gejo, T.; Harrison, J. A.; Huber, J. R. *J. Phys. Chem.* **1996**, *100*, 13941.
(24) Continetti, R. E.; Cyr, D. R.; Osborn, D. L.; Leahy, D. J.; Neumark, D. M. *J. Chem. Phys.* **1993**, *99*, 2616.
(25) Sidis, V. *J. Phys. Chem.* **1989**, *93*, 8128.
(26) Demkov, Y. N. *Sov. Phys. JETP* **1964**, *18*, 138.
(27) Krems, M.; Zirbel, J.; Thomason, M.; DuBois, R. D. *Rev. Sci. Instrum.* **2005**, *76*, 7.
(28) Cave, R. J.; Newton, M. D. *Chem. Phys. Lett.* **1996**, *249*, 15.
(29) Goates, S. R.; Chu, J. O.; Flynn, G. W. *J. Chem. Phys.* **1984**, *81*, 4521.
(30) Dyakov, Y. A.; Mebel, A. M.; Lin, S. H.; Lee, Y. T.; Ni, C. K. *J. Phys. Chem. A* **2007**, *111*, 9591.
(31) Heikkila, A. T.; Lundell, J. *J. Phys. Chem. A* **2000**, *104*, 6637.

JP901462D